J Mater Sci: Mater Med (2008) 19:1559–1563
DOI 10.1007/s10856-008-3373-x

Preparation of tricalcium phosphate/calcium pyrophosphate structures via rapid prototyping

Uwe Gbureck · Tanja Hölzel · Isabell Biermann · Jake E. Barralet · Liam M. Grover

Received: 30 August 2007 / Accepted: 4 January 2008 / Published online: 31 January 2008

Abstract Custom made tricalcium phosphate/calcium pyrophosphate bone substitutes with a well-defined architecture were fabricated in this study using 3D powder printing with tricalcium phosphate (TCP) powder and a liquid phase of phosphoric acid. The primary formed matrix of dicalcium phosphate dihydrate (DCPD, brushite) was converted in a second step to calcium pyrophosphate (CPP) by heat treatment in the temperature range 1,100–1,300°C. The structures exhibited compressive strengths between 0.8 MPa and 4 MPa after sintering at 1,100–1,250°C, higher strengths were obtained by increasing the amount of pyrophosphate formed in the matrix due to a post-hardening regime prior sintering as well as by the formation of a glass phase from TCP and calcium pyrophosphate above 1,280°C, which resulted in a strong densification of the samples and compressive strength of >40 MPa.

1 Introduction

Calcium phosphate (CaP) ceramics have been widely used as bone grafts in orthopaedics and dentistry [1–3]. Most of these materials are based upon calcium salts of orthophosphoric acid (H_3PO_4), e.g., tricalcium phosphate ($Ca_3(PO_4)_2$; TCP) [4], hydroxyapatite ($Ca_5(PO_4)_3OH$) [5] or brushite ($CaHPO_4{\cdot}2H_2O$) [6]. Variations in CaP composition can lead to different dissolution/precipitation behaviour and may therefore also affect the bone response. Besides orthophosphates, condensed phosphates like pyrophosphate ($P_2O_7^{4-}$) or even polyphosphates ($P_nO_{3n+1}^{(n+2)-}$) are attractive for bone replacement since these ions are present in serum [7] (1.8 μM $P_2O_7^{4-}$) and are thought to participate in the bone mineralisation process [8]. Polyphosphates are present in the body as compounds such as adenosine triphosphate (ATP), which are essential to metabolism [9].

Calcium pyrophosphate ceramics are traditionally processed by sintering secondary phosphates like brushite or monetite ($CaHPO_4$; DCPA) following a slip casting or isostatic-pressing regime to produce the desired shape. This processing limitation means that it is only possible to produce regular geometries, e.g., cylinders or cuboids, and it is difficult to produce custom made implants which would exactly fill a bone defect. In this work we describe the manufacture of custom-made calcium pyrophosphate implant structures and scaffolds via a free form rapid prototyping process. Fabrication of irregular samples was performed with a commercial 3D-powder printing system using a calcium phosphate cement setting reaction, which produces a matrix of brushite from TCP powder and diluted acidic orthophosphate solution as the liquid printing phase. In a second step, these matrices were converted to α-calcium pyrophosphate during sintering at temperatures of 1,000–1,300°C maintaining the shape of the implants. The mechanical performance and porosity contained within the ceramic samples were characterised and their phase composition was determined using X-ray diffraction (XRD) analysis.

U. Gbureck (✉) · T. Hölzel · I. Biermann
Department for Functional Materials in Medicine and Dentistry, University of Würzburg, Pleicherwall 2, 97070 Wurzburg, Germany
e-mail: uwe.gbureck@fmz.uni-wuerzburg.de

J. E. Barralet
Faculty of Dentistry, McGill University, Strathcona Anatomy and Dentistry Building, 3640 University St., Montreal, QC, Canada H3A 2B2

L. M. Grover
Chemical Engineering, University of Birmingham, Edgbaston, Birmingham B15 2TT, UK

2 Materials and methods

TCP was synthesized by heating a mixture of monetite (Merck, Darmstadt, Germany) and calcium carbonate (Merck, Darmstadt, Germany) (Ca:P = 1.5) to 1,400°C for 7 h followed by quenching to room temperature. The sintered cake was crushed with a pestle and mortar and passed through a 160 μm sieve and then ground in a ball mill (PM400, Retsch, Haan, Germany) for 10 min to a mean particle size of 30 μm.

Printing of cement samples was performed with a 3D-powder printing system (Z-Corporation, Burlington, MA, USA) using the TCP powder and diluted phosphoric acid (Merck, Darmstadt, Germany) with different concentrations in the range 5–30%. Approximately 9 kg (3 batches) of TCP powder were filled into the printer and manually compressed using hand pressure and a metal plate (with bore holes) provided by the manufacturer. The powder bed for the printed samples was prepared in the same way using 1 kg TCP powder. Printing was performed with the following parameters: 100 μm layer thickness, binder/volume ratio of 0.28 (shell) and 0.14 (core) with a saturation level of 89%. An additional post-hardening regime was performed by immersing samples in 20% phosphoric acid for 30 s following drying in air for 1 h. This procedure was repeated twice.

Samples were thermally treated after printing at temperatures between 1,100°C and 1,300°C for 5 h. Cylindrical samples (diameter 10 mm × height 20 mm) for compressive strength testing were tested in axial compression at a crosshead speed of 1 mm/min using a static mechanical testing machine (440, Zwick, Ulm, Germany) and a 5 kN load cell. Diametral tensile strengths (DTS) were determined using cylinders of 10 mm diameter and 5 mm height with a cross-head speed of 10 mm/min. The DTS was calculated from DTS (MPa) = $2F_{max}/(\pi * d * h)$, where d = diameter (10 mm), h = height of the sample (5 mm) and F_{max} is the failure load. The apparent density of the samples was calculated by using measured dimensions and weights. X-ray diffraction patterns of set cements were recorded on an X-Ray diffractometer (D5005, Siemens, Karlsruhe, Germany). Data were collected from $2\theta = 20–40°$ with a step size of 0.02° and a normalized count time of 1 s/step. The presence of α-TCP, β-TCP and α-calcium pyrophosphate in the bone substitutes was confirmed by comparing the complete patterns with published data [10–12]. The relative porosity contained within the cement matrices was determined using the Archimedes method. The fracture surfaces of the failed cement samples were examined using a scanning electron microscope (5300 LV, JEOL, Tokyo, Japan).

3 Results

The printing process enabled the production of complex components with an x-y-z resolution of ± 200 μm as shown in Fig. 1. Following printing, the ceramic matrices consisted of a combination of β-TCP and brushite (Fig. 2). As the matrices were heated to 1,250°C α-calcium pyrophosphate (α-CPP) was detected, with a concurrent reduction in the intensity of peaks indicative of brushite. Further heating of the ceramic to 1,300°C resulted in the disappearance of peaks symptomatic of α-CPP, suggesting the formation of a glass between TCP and α-CPP. At the same time, the compressive strength exhibited by the materials decreased with temperature treatment from 6 MPa to 0.8–4 MPa (Fig. 3), which was associated with a small decrease in the density of the material (Fig. 4) and a shrinkage of the samples of approximately 2–4% (Table 1). At higher temperatures of 1,300°C, both a strong increase of the strength to 25–45 MPa and of the apparent density to 2.3–2.7 g/cm^3 was observed for samples printed with 5% or 10% H_3PO_4 (Fig. 4). The increase in the apparent density was associated with a marked reduction in relative porosity from 39 ± 4% to 16 ± 1%.

To increase the amount of calcium pyrophosphate in the sintered samples, the degree of conversion to brushite (which forms CPP during heat treatment) was increased after printing by a post-hardening regime immersing the samples in 20% phosphoric acid for up to 3 × 30 s. The post-hardening regime increased the compressive strength exhibited by the non-heat treated samples by almost tenfold to a maximum of 24.9 ± 4.3 MPa following treatment in phosphoric acid for 3 × 30 s. This increase in compressive strength was associated with a marked reduction in relative porosity from 39 ± 4% to 27 ± 3% (Table 2B). Although sintering resulted in a reduction in compressive strength and generally resulted in an increase in porosity, post-hardening the sintered samples in phosphoric acid resulted

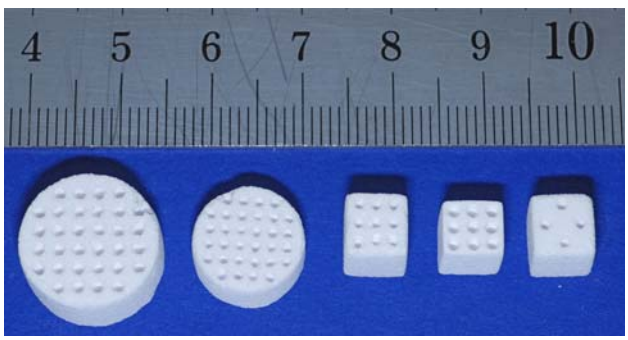

Fig. 1 Macroporous calcium pyrophosphate/tricalcium phosphate monoliths formed by 3D powder printing and sintering at 1,200°C (scale in cm)

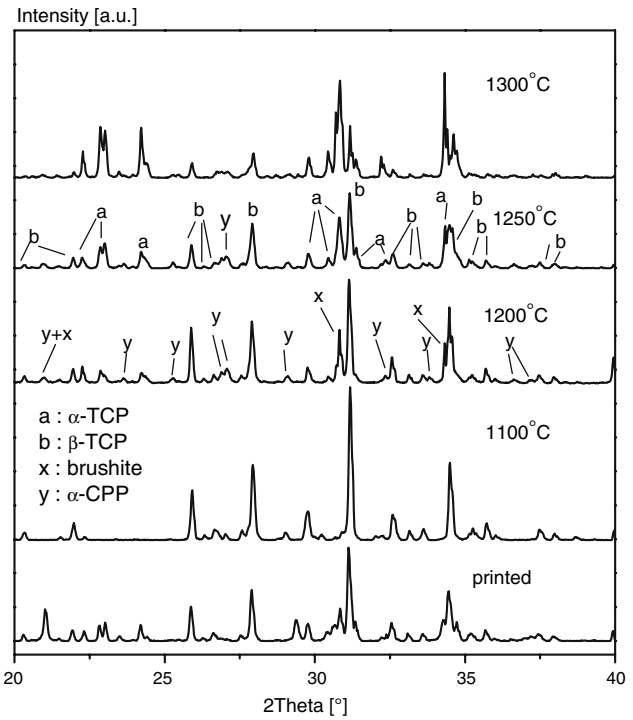

Fig. 2 X-ray diffraction patterns of samples printed with 20% phosphoric acid as binder after heat treatment at various temperatures

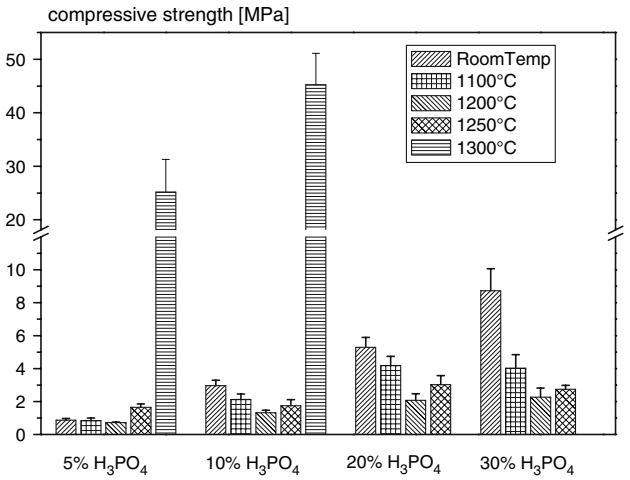

Fig. 3 Compressive strength of samples printed with different H_3PO_4 concentrations following additional sintering at various temperatures; error bars are standard deviations ($n = 7$)

in an increase in compressive strength from 2.6 ± 0.2 MPa to 5.9 ± 0.5 MPa. Prior to heat treatment, the cement matrix consisted of irregular shaped particles of 30–60 μm in diameter encrusted in submicron irregular particles (Fig. 5a). Following sintering at 1,200°C for 5 h, the ceramic microstructure consisted of fewer discernible particles, which had become adjoined at their interfaces (Fig. 5b).

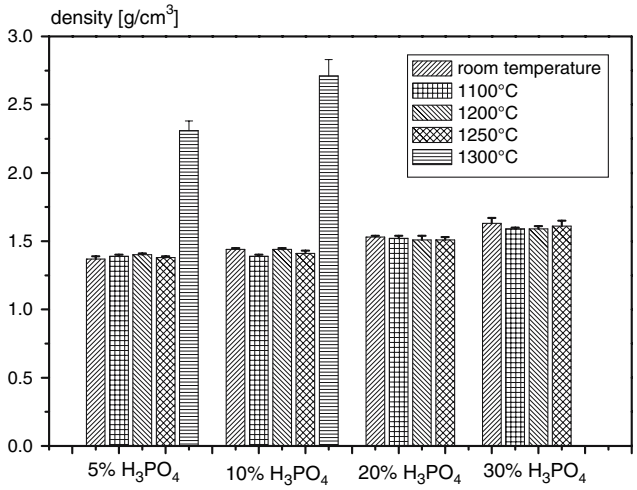

Fig. 4 Density of samples printed with different H_3PO_4 concentrations and additional sintering at various temperatures; error bars are standard deviations ($n = 7$)

4 Discussion

Variations in CaP composition can lead to different dissolution/precipitation behaviour and may therefore also affect the bone response. Pyrophosphate based biomaterials are attractive for bone replacement since $P_2O_7^{4-}$ ions are thought to participate in the bone mineralisation process [7, 8]. One of the first reports of sintered dicalcium pyrophosphate as a biomaterial was that of Kitsugi et al. [13] who showed that after 10 weeks of implantation the sintered dicalcium pyrophosphate had formed a bond with bone. Other studies have shown that sintered dicalcium pyrophosphate is more rapidly resorbed in vivo than sintered hydroxyapatite. When implanted in rabbit femoral condyles it was shown that sintered β-dicalcium pyrophosphate containing pores of 100 μm and 400 μm (pore fraction 48.3%) facilitated complete bone ingrowth after a period of 4 weeks and after 8 weeks was resorbed by a process of dissolution and phagocytosis leaving a newly formed bone structure [14].

Traditional preparation of calcium pyrophosphate ceramics involve the heat treatment of slip-casted or isostatically pressed calcium phosphate materials with a Ca/P ratio in the range $1.0 < Ca/P < 1.5$. Processing of calcium pyrophosphate/tricalcium phosphate green bodies with defined macroporous architecture was done in this study using 3D powder printing as a rapid prototyping technology. Various authors have described rapid prototyping techniques to fabricate hydroxyapatite or tricalcium phosphate scaffolds for bone repair or tissue engineering [13–18], mostly by using polymeric binder systems which were then removed by sintering. The preparation of TCP/CPP samples is this study was done by using an inorganic

Table 1 Medium dimensional changes and standard deviations ($n = 7$) of samples during heat treatment; samples were printed with either 5% or 10% phosphoric acid as binder

Temperature	H_3PO_4 conc. (%)	Dimensions (mm) and shrinkage (%)		
		H	r_{min}	r_{max}
No heat treatment	5	20.44 ± 0.08	4.94 ± 0.04	5.05 ± 0.05
1,200°C/5 h		20.25 ± 0.09	4.8 ± 0.04	4.91 ± 0.03
		(0.93)	(2.8)	(2.8)
1,250°C/5 h		20.26 ± 0.05	4.76 ± 0.06	5.04 ± 0.05
		(0.9)	(3.6)	(0.2)
1,300°C/5 h		17.23 ± 0.29	3.91 ± 0.06	4.32 ± 0.04
		(15.7)	(20.9)	(14.6)
No heat treatment	10	20.76 ± 0.06	4.96 ± 0.02	5.18 ± 0.02
1,200°C/5 h		20.19 ± 0.09	4.84 ± 0.11	5.07 ± 0.14
		(2.7)	(2.4)	(2.1)
1,250°C/5 h		20.35 ± 0.12	4.87 ± 0.05	5.2 ± 0.14
		(1.9)	(1.8)	(–)
1,300°C/5 h		16.32 ± 0.27	3.82 ± 0.03	4.16 ± 0.16
		(21.4)	(22.9)	(19.7)

Table 2 (A) Compressive strength (CS) and diametral tensile strength (DTS) of structures printed with 10% H_3PO_4 following post-hardening in 20% acid for up to 3 × 30 s and additional sintering at 1,200°C for 5 h and (B) the porosity contained within the ceramic matrices ($n = 7$)

(A) Post-hardening	Before sintering		After sintering	
	CS (MPa)	DTS (MPa)	CS (MPa)	DTS (MPa)
–	2.81 ± 0.27	0.60 ± 0.08	2.56 ± 0.15	0.37 ± 0.03
1 × 30 s	22.4 ± 5.8	4.16 ± 0.47	6.91 ± 1.22	1.03 ± 0.21
2 × 30 s	24.9 ± 3.5	4.44 ± 0.62	6.88 ± 1.00	0.98 ± 0.13
3 × 30 s	24.9 ± 4.3	4.38 ± 0.76	5.91 ± 0.47	0.92 ± 0.15

(B) Post-hardening	Before sintering	After sintering
	Porosity (%)	Porosity (%)
–	39 ± 4	42 ± 5
1 × 30 s	37 ± 4	38 ± 3
2 × 30 s	32 ± 2	42 ± 5
3 × 30 s	27 ± 3	30 ± 2

binder in a two step process. Firstly, tricalcium phosphate powder reacted with phosphoric acid which formed a matrix of dicalcium phosphate dihydrate (brushite) in accordance with Eq. 1:

$$Ca_3(PO_4)_2 + H_3PO_4 + 6H_2O \rightarrow 3CaHPO_4 \cdot 2H_2O \quad (1)$$

A second step was the heat treatment of the printed structures which led to a thermal decomposition of the brushite phase and forms α-calcium pyrophosphate in accordance Eq. 2:

$$2CaHPO_4 \cdot 2H_2O \rightarrow \alpha\text{-}Ca_2P_2O_7 + 5H_2O \quad (2)$$

The mechanical performance of sintered CPP ceramics was comparatively low for sintering temperatures up to 1,250°C, compressive strengths found in this study were approx. 2–3 MPa depending on the phosphoric acid concentration used for printing, which corresponds to the amount of α-CPP formed during sintering. The reduction in compressive strength with heat treatment could be explained by the formation of porosity within the ceramic structure (Table 2B) during heating. The density of α-CPP is considerably higher than brushite (2.95 g/cm^3 [12] compared with 2.32 g/cm^3) and consequently during conversion the ceramic matrix would have undergone a significant shrinkage.

Strength improvements were obtained by two different ways. Firstly, a post-hardening regime prior to sintering by immersing the samples in diluted phosphoric acid gave a

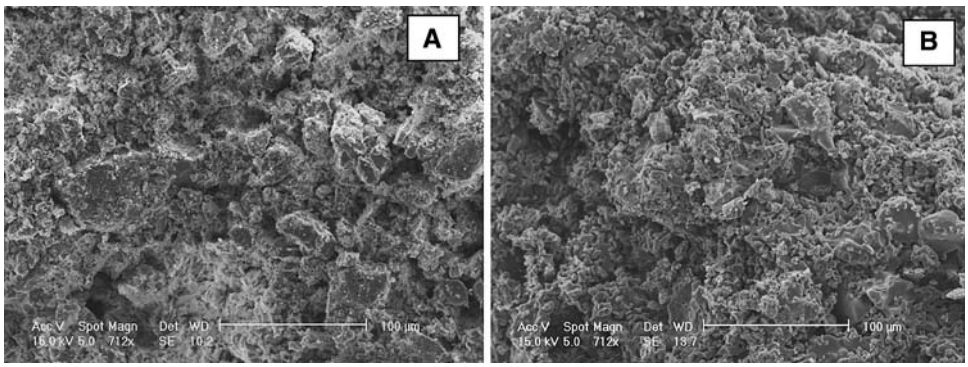

Fig. 5 Scanning electron micrographs of calcium pyrophosphate ceramic fracture surfaces (**a**) Prior to heat treatment and (**b**) following 5 h sintering at 1,200°C

100% increase in mechanical performance with maximum compressive strength of 5–6 MPa, which is a result of a higher amount of calcium pyrophosphate formed during sintering. Secondly, higher sintering temperatures of 1,300°C resulted in a strong densification of the samples with an increase of the compressive strength to more than 40 MPa. This behaviour can be explained by the formation of a glass phase in the pore structure of the material from α-CPP and tricalcium phosphate according to the phase diagram [19], however this procedure only worked well for cements with comparatively low pyrophosphate contents e.g., samples printed with 5% or 10% phosphoric acid. The production of ceramics containing a higher proportion of α-CPP resulted in a loss of the sample morphology due to melting.

5 Conclusion

Here we have demonstrated that it is possible to fabricate calcium pyrophosphate ceramics of defined architecture heat-treating 3D printed brushite cements. Although heat treatment of the cements to 1,200°C resulted in considerable weakening of the matrix, further heating to 1,300°C caused a significant densifiction of the ceramic by the formation of a glassy calcium phosphate–pyrophosphate phase and the production of a material that exhibited a compressive strength of 40 MPa. 3D printing and heat treatment could therefore result in the manufacture of bespoke α-CPP implants for bone replacement applications.

References

1. S.V. Dorozhkin, M. Epple, Angew. Chem. Int. Ed. **41**, 3130 (2002)
2. R.Z. Legeros, *Calcium Phosphates in Oral Biology and Medicine* (Karger, Basel, 1991)
3. M. Bohner, Eur. Spine J. **10**, 114 (2001)
4. P.S. Rosen, M.A. Reynolds, G.M. Bowers, Periodontology **22**, 88 (2000)
5. L.L. Hench, J. Am. Ceram. Soc. **81**, 1705 (1998)
6. A.A. Mirtichi, J. Lemaitre, E. Munting, Biomaterials **10**, 634 (1989)
7. R.I. Martin, P.W. Brown, Biomaterials **5**, 96 (1994)
8. L. Hessle, K.A. Johnson, H.C. Anderson, R. Terkeltaub, J.L. Millan, J. Bone Miner. Res. **17**, S128 (2002)
9. E. Fosslien, Ann. Clin. Lab. Sci. **31**, 25 (2001)
10. M. Mathew, L.W. Schroeder, B. Dickens, W.E. Brown, Acta Crystallog. B. **33**, 1325 (1977)
11. B. Dickens, L.W. Schroeder, W.E. Brown, J. Solid State Chem. **10**, 232 (1974)
12. C. Calvo, Inorg. Chem. **7**, 1345 (1968)
13. T. Kitsugi, T. Yamamuro, T. Nakamura, S. Kotani, T. Kokubo, H. Takeuchi, Biomaterials **3**, 216 (1993)
14. Z. Sadeghian, J.G. Heinrich, F. Moztaradeh, CFI-Ceram. Forum Int. **81**, E39 (2004)
15. C.E. Wilson, J.D. De Bruijn, C.A. Van Blitterswijk, A.J. Verbout, W.J.A. Dhert, J. Biomed. Mater. Res. **68A**, 123 (2004)
16. N.K. Vail, L.D. Swain, W.C. Fox, T.B. Aufdlemorte, G. Lee, J.W. Barlow, Mater. Des. **20**, 123 (1999)
17. K.H. Tan, C.K. Chua, K.F. Leong, C.M. Cheah, P. Cheang, M.S. Abu Bakar, S.W. Cha, Biomaterials **24**, 3115 (2003)
18. C.K. Chua, K.F. Leong, K.H. Tan, F.E. Wiria, C.M. Cheah, Biomaterials **15**, 1113 (2004)
19. J.C. Elliott, *Structure and Chemistry of the Apatites and Other Calcium Orthophosphates* (Elsevier, Amsterdam, 1994), p. 49